

## Review article

## Open Access

Youjun Zeng<sup>a</sup>, Rui Hu<sup>a</sup>, Lei Wang, Dayong Gu, Jianan He, Shu-Yuen Wu, Ho-Pui Ho, Xuejin Li, Junle Qu, Bruce Zhi Gao and Yonghong Shao\*

# Recent advances in surface plasmon resonance imaging: detection speed, sensitivity, and portability

DOI 10.1515/nanoph-2017-0022

Received February 4, 2017; revised March 30, 2017; accepted April 2, 2017

**Abstract:** Surface plasmon resonance (SPR) biosensor is a powerful tool for studying the kinetics of biomolecular interactions because they offer unique real-time and label-free measurement capabilities with high detection sensitivity. In the past two decades, SPR technology has been successfully commercialized and its performance has continuously been improved with lots of engineering efforts. In this review, we describe the recent advances in SPR technologies. The developments of SPR technologies focusing on detection speed, sensitivity, and portability are discussed in details. The incorporation of imaging techniques into SPR sensing is emphasized. In addition, our SPR imaging biosensors based on the scanning of wavelength by a solid-state tunable wavelength filter are highlighted. Finally, significant advances of the vast developments in nanotechnology-associated SPR sensing for sensitivity enhancements are also reviewed. It is hoped

that this review will provide some insights for researchers who are interested in SPR sensing, and help them develop SPR sensors with better sensitivity and higher throughput.

**Keywords:** biosensors; surface plasmon resonance; SPR imaging; nanoplasmonics; plasmonics.

## 1 Introduction

Surface plasmon resonance (SPR) biosensors have become an important tool for exploring the kinetics of biomolecular interactions, and have been widely adopted in the detection of chemical and biological analytes [1]. Moreover, by combining the SPR technique with an imaging system, one can readily achieve high-throughput real-time label-free biosensing in two-dimensional (2D) microarrays and parallel monitoring of multiple numbers of biomolecular interactions. In the past few decades, it has been widely used for measuring specificity, affinity, and kinetic parameters in the macromolecule binding process, such as protein-protein, protein-DNA, receptor-drug, and cell/virus-protein bindings [2]. To date, four practical SPR sensing techniques, involving intensity, wavelength, angle, and phase interrogations, have been widely reported [3]. In the intensity interrogation SPR, the shift of the SPR dip is translated into the change of reflectivity in the linear region of the SPR angular or spectral response curve. In the wavelength interrogation mode, the SPR spectral profile can be obtained by either scanning the incidence wavelength or using a spectrometer for analyzing the reflected beam. In the angular interrogation mode, the shift of the SPR dip can be monitored by continuous scanning of the SPR angular spectrograph. In the phase interrogation mode, the SPR phase shift can be measured by detecting the phase difference between the signal beam and reference beam. To satisfy the requirements of high throughput, real time, and high sensitivity in the detection of chemical and biological analytes, many

<sup>a</sup>**Youjun Zeng and Rui Hu:** These authors contributed equally to this work.

**\*Corresponding author: Yonghong Shao,** Key Laboratory of Optoelectronic Devices and Systems of Ministry of Education and Guangdong Province, College of Optoelectronic Engineering, Shenzhen Key Laboratory of Sensor Technology, Shenzhen University, Shenzhen 518060, China, Tel.: +86-135-2884-9905, e-mail: shaoyh@szu.edu.cn

**Youjun Zeng, Rui Hu, Lei Wang, Xuejin Li and Junle Qu:** Key Laboratory of Optoelectronic Devices and Systems of Ministry of Education and Guangdong Province, College of Optoelectronic Engineering, Shenzhen Key Laboratory of Sensor Technology, Shenzhen University, Shenzhen 518060, China

**Dayong Gu and Jianan He:** Shenzhen Entry-exit Inspection and Quarantine Bureau, Shenzhen 518033, China

**Shu-Yuen Wu and Ho-Pui Ho:** Department of Electronic Engineering, The Chinese University of Hong Kong, Shatin, Hong Kong

**Bruce Zhi Gao:** Department of Bioengineering and COMSET, Clemson University, Clemson, SC 29634, USA

efforts have been made. More recently, owing to the vast developments in nanotechnology, many new ideas involving nanostructures in SPR sensing have emerged and shown lots of advancements. The emergence of new SPR techniques based on the above principles has served as a promising sensing approach in the monitoring of small-molecule interactions. In this review, we present some of the latest advances and developments in this field, focusing on the technical design of different SPR sensing techniques. New advancements in four practical SPR sensing techniques are introduced, followed by a brief introduction to recent technical advancements in nanostructure-based SPR sensing techniques.

## 2 Intensity interrogation SPR

In the intensity interrogation mode, the shift of the SPR dip can be monitored by measuring the change of reflectivity in the linear region of the SPR angular or spectral response curve. In the linear region, the change of the SPR signal is proportional to the change of the refractive index above the metallic film. This requires both the incidence angle and wavelength of excitation light to be fixed and optimized for best possible sensitivity. In order to improve the measurement throughput, multichannel SPR [4, 5] and SPR imaging (SPRi) [6, 7] are developed. Figure 1 shows a typical scheme of a prism-based intensity interrogation SPRi setup. The charge-coupled device (CCD) camera records a series of 2D intensity contrast images of the sensor surface in real time. Each pixel within the image frame provides one data point of the SPR response in the sensor surface. Theoretically, this one-to-one correspondence between the sensor surface and the 2D CCD imaging pixel arrays may offer massively parallel fast biosensing capability. However, in prism-based

SPRi, the spatial resolution is significantly low, especially along the direction parallel to the surface plasmon wave (SPW) due to the geometrical aberration of the prism and the propagating length of the SPW. An optimized spatial resolution of  $1.7\ \mu\text{m}$  perpendicular and  $2.8\ \mu\text{m}$  parallel to the SPW has been obtained [8]. So far, the intensity interrogation mode is a straightforward case for 2D arrays. It has been widely used and commercialized by Biacore GE and GWC Technologies for high-throughput analysis in immunosensing [4], DNA hybridization [7], protein interactions [9–11], and cellular analysis [12, 13]. However, for the detection of multiple interactions simultaneously, it is usually not practical to obtain a homogeneous and optimal response over the entire analyzed surface with the choice of a unique operating point [14].

## 3 Angle interrogation SPR

In the angular interrogation mode, the incidence wavelength is fixed and the shift of the SPR dip can be monitored by continuous scanning of the SPR angular spectrograph. As compared to the intensity interrogation mode, the noise of the light source could be eliminated in the angle interrogation mode, which results in a relatively higher sensitivity [15]. In a conventional angle interrogation SPR sensor, a goniometer with two rotational stages is usually required when scanning the angle of incidence. To avoid using an expensive goniometer, Mohanty and Kasiviswanathan proposed a two-prism setup with only one rotating element [16]. In such a setup, the emergent rays are always parallel to each other with minimal separation. More importantly, the rays fall normally on the detector for a wide angular scanning range, thus providing a relatively large dynamic range. Sathiyamoorthy et al. then modified the two-prism setup to keep both the interrogation spot and the reflected beam stationary [17]. Although the two-prism configuration have reduced the rotational stage from two to one and thus improved the sensitivity, to get a faster response, it is ideal to avoid any mechanical movements. For such a purpose, a convergent light beam covering an interval of incidence angles is usually introduced. The resonance angle can then be obtained with a detector array by curve fitting the reflectance minimum [18]. However, in such configurations, to increase the angle detection resolution for sensitivity improvements requires a lot of efforts. Tao et al. have achieved a high resolution of  $\sim 10^{-5}$  deg and a fast response time of  $1\ \mu\text{s}$  using a bicell photodetector for accurate measurement of shift in the SPR angle [19]. Berger and Greve [20] introduced

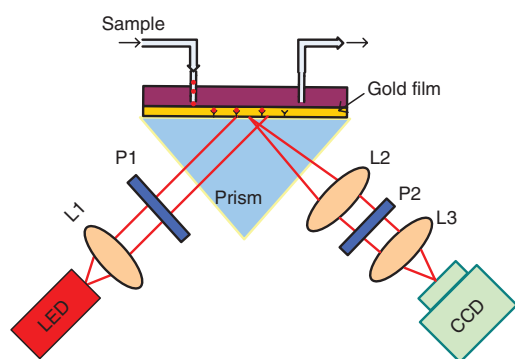


**Figure 1:** Schematic illustration of a typical prism-based intensity interrogation SPRi setup.

differential detection in their setup, where the angle of incidence was modulated by a piezoelectric actuator and the reflectance signal was measured with a lock-in amplifier. Their sensor has shown a sub-microdegree resolution for the detection of immunoreaction.

A single-spot interrogation SPR sensor can detect biological response with high sensitivity; however, it is not satisfactory in terms of achieving high-throughput measurements. This is when imaging technology comes in. Wolf et al. [21, 22] developed a prism- and detection-arm-rotated angle-resolved SPRi for quantitative characterization of DNA interactions and the kinetics of DNA-drug binding. White light from a tungsten-halogen source was used for SPR excitation, and a liquid crystal variable retarder was employed to correct images for spatial intensity variation in the light source. With such corrections, the authors achieved accurate measurements of surface coverage without the need for instrumental calibration. In 2008, Ruemmele et al. [23] reported an inexpensive automated angle-scanning SPRi instrument with optimum flexibility. So far, angle-resolved SPRi has been widely applied for biomolecular interaction detection with high-throughput. Beusink et al. demonstrated the use of a commercial SPRi instrument for sensitive, accurate, and label-free detection of analytes with different molecular weights in a large dynamic range (from 2.4 to 150 kDa) within the same experiment [24]. In another angle scanning SPRi device developed by Zhou et al. [25] a rhombic structure was introduced to convert the linear motion of a piezoceramic motor into the angular motion of the laser and CCD arrays, as shown in Figure 2. Owing to the fast scanning speed provided by the piezoceramic

motor, the authors could detect the mismatched bases in the caspase-3 DNA at high throughput. In order to avoid the mechanical scanning of the detection arm, angle-resolved SPRi technologies based on an angle-controlled mirror or an acousto-optic deflector have been developed [2, 24]. Therefore, the measurement rate of the SPR dip is improved up to 10 Hz in the angle-resolved SPRi [2].

## 4 Wavelength interrogation SPR

In the wavelength interrogation mode, the angle of incidence is fixed while the SPR spectral profile is continuously obtained to monitor the SPR dip. Wavelength interrogation SPR provides a wide dynamic range, and its detection sensitivity could be as high as that offered by angle interrogation. Moreover, wavelength interrogation-based SPR sensors are much more flexible in terms of optimization because the operation wavelength range can be easily tuned to achieve the best SPR excitation. In this mode, the SPR spectral profile can be obtained by either scanning the incidence wavelength or using a spectrometer for analyzing the reflected beam. In recent years, lots of efforts have been spent to improve the sensitivity as well as the throughput. Yuk et al. [26] introduced an SPRi sensor for the investigation of protein interactions on arrays, where, in addition to the calculation of the resonance wavelength from the SPR reflectivity spectra, the authors also incorporated the position control. With these arrangements, they could quantitatively analyze the specific binding of anti-Rac1 and anti-RhoA to Rac1 and RhoA on the protein arrays. In addition to high throughput, it is also important to achieve real-time monitoring of biological interactions. To improve the time resolution, Liu et al. [27] reported a 1D optical line scan spectral SPR system for imaging 2D arrays. It took the system 60 s to measure the SPR dips of the 2D array for an area of  $8 \times 8$  mm. Recently, to further speed up the measurements, an optimized algorithm based on five parameters was developed for spectral SPRi sensors, with which the measurement time of the SPR dip was reduced dramatically to 10 s for 2D arrays [14].

Our group also built a fast-wavelength interrogation SPRi system, as shown in Figure 3 [28]. The system has a halogen lamp as the excitation source, while a liquid crystal tunable filter (LCTF) was used for fast incident wavelength scanning with a bandwidth of 8 nm. The reflected light is captured by a 12-bit CCD. With this system, we have achieved a sensitivity of  $4.69 \times 10^{-6}$  refractive index units (RIU) and a dynamic range of  $5.55 \times 10^{-2}$  RIU. Using a feedback loop, the scanning wavelength

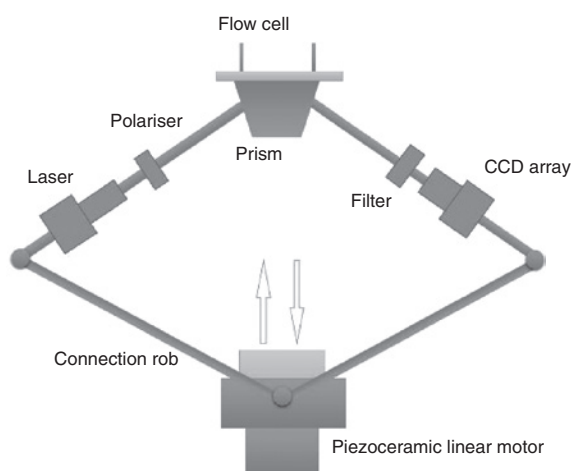


**Figure 2:** Schematic of a rhombic-shaped angle interrogation SPRi system based on a piezoceramic motor. Reprinted with permission from Ref. [25].

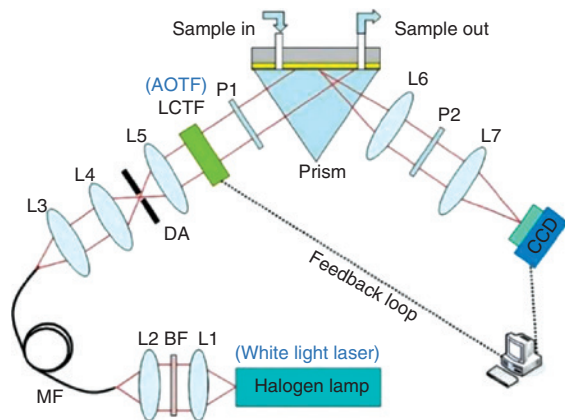


**Figure 3:** Schematic of our feedback loop-based imaging wavelength SPR system in the Kreschmann configuration. L1, L2, L3, L4, L5, L6, and L7, lenses; MF, multimode fiber; DA, diaphragm aperture; AOTF, acousto-optic tunable filter. P1 and P2, polarizers. Reprinted with permission from Ref. [28].

range was dynamically adjusted to match the SPR dip and thus to achieve a high scanning speed. With this technique, about 700 ms is required for one cycle of scanning [29]. According to a unified theoretical model proposed by Wong et al. [30] the sensitivity of the SPR sensor depends upon the noise of the used optoelectronic components as opposed to the design of the SPR optical platform. To improve the sensitivity of our system, the halogen lamp was then replaced with a white light laser, which has higher intensity, a more stable spectrum in the visible

range, and most importantly, a much lower noise level. To improve the scanning speed, the LCTF was replaced with an acousto-optic tunable filter, which is faster in switching the incident wavelength and also has a narrower output bandwidth. With such replacements, the sensitivity and dynamic range were improved to  $1.27 \times 10^{-6}$  RIU and  $4.63 \times 10^{-2}$  RIU, respectively. The time required for one cycle of scanning is reduced to 340 ms [31].

## 5 Phase interrogation SPR

The phase interrogation SPR technique requires a fixed angle of incidence and wavelength for the incident light while the phase of the reflected light is measured. Compared with the angle or wavelength interrogation mode, the phase interrogation mode is very suitable for integration with imaging technology to achieve high throughput, and it also provides a great potential for an ultrahigh sensitivity [15]. However, direct optical phase measurement is not as simple, as no detectors are fast enough to resolve the oscillating intensity of an optical beam. Thus, phase measurement normally relies on the interference between a signal beam and a reference beam, from which a low-frequency signal can be generated and resolved by a photodetector [32]. In 1996, Nelso et al. [33] proposed an SPR phase sensor based on optical heterodyne detection (Figure 4). An acousto-optic modulator (AOM) was used to divide the laser source into two beams with a frequency difference of

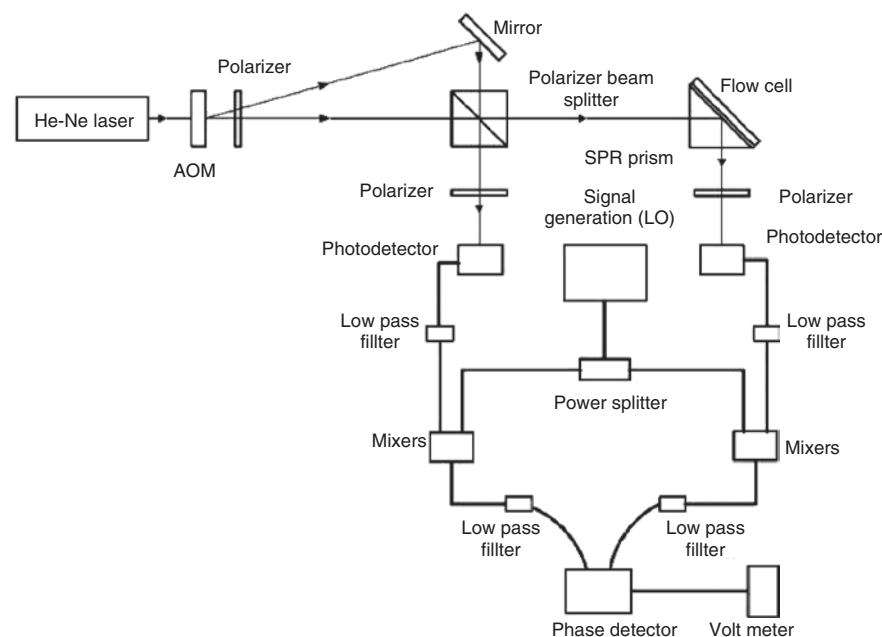


**Figure 4:** Schematic of phase detection sensing configuration with AOM. Reprinted with permission from Ref. [33].



140 MHz. Then, a polarizing splitter was used to generate the reference and signal light beams for the phase detection. With this setup, an accurate measurement of the SPR-generated phase shift was obtained, and the authors could achieve an ultrahigh sensitivity of up to  $5 \times 10^{-7}$  RIU. Following that, Xinglong et al. introduced a transverse Zeeman laser as the light source, which includes both p- and s-polarized light, and demonstrated a heterodyne phase detection SPR sensor for immunosensing [34]. Later on, Wu et al. reported another similar heterodyne phase detection sensor and pushed the sensitivity to  $2 \times 10^{-7}$  RIU [35]. Subsequently, by integrating the features of a common-path optical heterodyne interferometer and the amplitude-ratio detection mode, Chou et al. developed a paired surface plasma wave biosensor that had achieved a record-high detection sensitivity of up to  $10^{-9}$  RIU [36, 37]. Besides AOM, a photoelastic modulator (PEM) can also be used to modulate the laser frequency. Peng et al. developed a single-beam approach where the input beam is modulated by a PEM and the SPR-induced phase change was obtained by an analytical signal-processing algorithm [38]. This single-beam system was then used for real-time monitoring of biomolecule binding reactions with detection sensitivity up to  $6 \times 10^{-7}$  RIU or 15 ng/ml [39, 40].

In the phase interrogation mode, Mach-Zehnder and Michelson interferometers have been widely adopted to get the SPR-induced phase shift [15, 32]. Kabashin and Nikitin firstly reported the use of Mach-Zehnder interferometer for SPR sensing [41, 42]. The SPR-induced phase change could be obtained by analyzing the interference fringes and their spatial displacements. The system demonstrated a sensitivity threshold of  $4 \times 10^{-8}$  RIU. Wu et al. proposed a similar Mach-Zehnder interferometer-based SPR sensor, as shown in Figure 5 [43]. In their setup, a piezoelectric transducer was used to introduce a periodic linear phase shift to the reference light, and a Wollaston

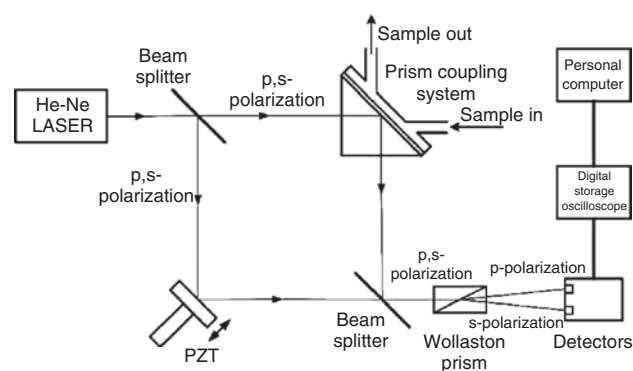


**Figure 5:** SPR phase sensor based on a Mach-Zehnder interferometer. Reprinted with permission from Ref. [43].

prism was used to extract the p- and s- polarization for the two detectors. The optimum sensitivity of the setup can achieve  $2 \times 10^{-8}$  RIU [44].

In general, a phase interrogation SPR sensor gives a higher sensitivity as compared to the angle or wavelength interrogation mode; however, the dynamic range is usually limited. In order to improve the detection dynamic range, Ng et al. [45] developed an optimized SPR biosensing system that had incorporated the temporal carrier technique with a common-path spectral interferometry. The system achieved a sensitivity of up to  $2 \times 10^{-8}$  RIU over a dynamic range of  $3 \times 10^{-2}$  RIU and was used for drug screening [46]. The phase interrogation mode can also be incorporated with the SPRi technique for high-throughput analysis. In 2000, Nikitin et al. [47] proposed a micro-array interferometry SPR biosensor for bio- and chemical sensing. Xinglong et al. [48] demonstrated a common-optical-path interferometry-based SPRi sensor combining SPR and spatial phase modulation measurement. The arrayed SPR sensor was then demonstrated for antigen-antibody binding and dissociation process with an improved sensitivity of  $>10^{-6}$  RIU [49, 50]. More recently, they have shown an improved system for protein microarray experiments with a wide dynamic range over 0.015 RIU and a sensitivity down to  $5 \times 10^{-7}$  RIU [51]. We also have proposed a wavelength-multiplexing phase-sensitive SPRi sensor, as shown in Figure 6 [52]. In this setup, a xenon lamp was used as the excitation source, followed by an LCTF to sweep the input wavelength and a liquid crystal modulator to modulate the optical retardation for phase dithering. An image sensor was used to capture the

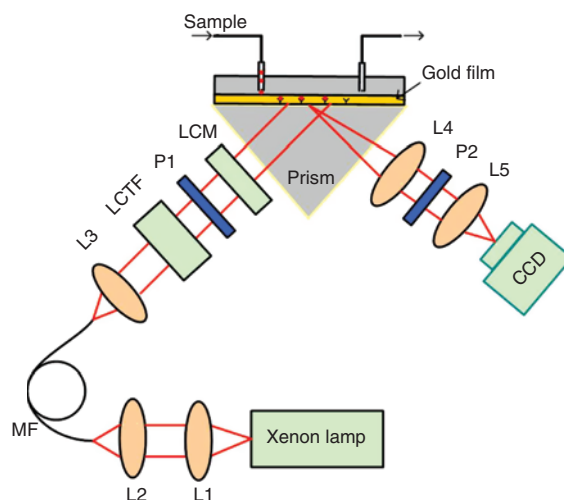


**Figure 6:** Phase-modulated SPR system. L1, L2, L3, L4, and L5, lenses; MF, multimode fiber; LCM, liquid crystal modulator. Reprinted with permission from Ref. [52].

intensity response of the sensor surface. With this system, we could find the SPR phase at any wavelength of interest, thus achieving a detection sensitivity of  $2.7 \times 10^{-7}$  RIU with a wide dynamic range of 0.0138 RIU.

## 6 Recent advances in nanoparticle- and nanomaterial-based SPR sensing

### 6.1 Plasmonic nanoparticle-based SPR sensing

With the developments in nanostructure engineering, nanotechnology has found many ways of enhancing the sensitivity of conventional SPR sensing techniques. Among these methods, one of the most commonly used strategies is the introduction of different metallic plasmonic nanostructures, especially those made of gold or silver. Typically, for a metallic nanostructure with a size in the range of several tens of nanometers or smaller, the free electrons were trapped on the nanoparticle surface. Under proper optical excitation, these free electrons would oscillate collectively in accordance with the incident light and thus results in localized SPR (LSPR). Similar to the conventional SPR, LSPR is also sensitive to the localized dielectric environment [53]. In addition, as the quantum size effect is involved in the LSPR effect, the size, shape, and composition of the metallic nanostructure would also affect the resonance dramatically. As for this plasmonic nanostructure-induced sensitivity enhancement, the key factor lies in the coupling between the surface plasmon polaritons (SPPs) from the conventional SPR sensor chip and the localized surface plasmon (LSP) from the plasmonic nanostructures.

Because of the facile way of synthesis and surface modification, gold and silver nanoparticles have been widely introduced into conventional SPR sensors to achieve ultrahigh sensitivity. Theoretically, the coupling between the LSP and SPP could be studied through various numerical models [54]. In a simulation shown by L  v  que and Martin, the coupling between the LSP and the SPP can produce a dramatic enhancement of the electromagnetic (EM) field by a factor of up to 5000 in the space between the nanoparticles and the plasmonic film [55, 56]. Moreover, according to a recent report from Li et al. when plasmonic nanoparticles are introduced into a conventional Kretschmann-Raether configuration for SPR sensing, the LSPs will be excited through extended surface plasmons

(ESPs). Owing to the strong confinement of the ESP waves in the vertical direction, the EM field between the plasmonic film and the nanoparticles could be enhanced at a much higher level (1–3 orders higher) than that directly excited from free space [57]. Although the numerical simulation could be straightforward, one should still pay attention to certain details. As an example, Golden et al. pointed out that the dielectric function of gold nanoparticles is not only wavelength dependent, which is well understood, but also dependent on the particle-to-metal-substrate distance in an angle-resolved SPRi configuration. It would be necessary and important to take these details into consideration in simulations [58].

Based on the LSP-SPP coupling-induced enhancement, many ultrasensitive biometric detectors for sensing subtle environmental changes have been demonstrated since the late 1990s [59–63]. In the LSP-SPP coupling configuration, numerical simulation shows that the EM field enhancement is usually the strongest in the gap between the nanoparticle and the film. To get an optimized sensitivity enhancement, it is important to put the analyte into the gap to induce perturbation, and this in most cases requires a sandwich configuration. In the past decades, various techniques making use of different parameters, which include the gap distance between the nanoparticle and the metal film and the physical properties of the nanoparticles, have been developed and optimized based on this phenomenon [64]. The colloidal synthesis of rod-shaped gold nanoparticles (nanorods) has offered another dimension of tunability than spherical ones. The gold nanorods have two LSPR wavelength peaks, of which the longitudinal LSPR-induced peak could be fine-tuned over a large range by changing its aspect ratio [65]. This has thus given us the opportunity to optimize the coupling efficiency between the LSP and SPP in the nanoparticle-film configuration. In this regard, we had demonstrated the use of functionalized gold nanorods as amplification labels for ultrasensitive SPR biosensing with a sensitivity estimated to be  $\sim 40$  pg/ml for antibody detection [66]. More recently, a similar ultrasensitive sandwich immunoassay setup was introduced for the tumor necrosis factor- $\alpha$  antigen detection in cancer-related disease research, while the detection limit of the antigen concentration was further pushed to the femtomolar range [61]. The same report has indicated that the orientation of gold nanorods toward the gold film is also a factor for the sensitivity enhancement. For further investigation, Kwon et al. [67] have made a detailed comparison over the nanoparticle size and shape. In their study, different gold nanoparticle shapes (cubic cages, rods, and quasi-spherical) were

systematically compared through thrombin detection. They found that the greatest enhancement in signal was observed for the quasi-spherical particles with the detection of thrombin concentrations as low as  $\sim 1$  aM, followed by the nanorods where  $\sim 10$  aM was detected. It is worth mentioning that the size of all the nanoparticles were in the range of 40–50 nm, which was proved to be more efficient than smaller nanoparticles. In general, the sandwich configuration for maximum sensitivity enhancement usually requires careful design and modifications of the gold film and/or the nanoparticle surface, which leads to complications of the SPR chip. To break this restriction, Maurer et al. [68] introduced a graphene spacer between the gold film and the nanoparticles. Their numerical simulations suggested that the LSP mode of the gold nanoparticles is dipolar and that the hotspots of the electric field are pushed to the top corners of the nanoparticles, which represents a 33% gain in sensitivity and opens up new sensing strategies.

Although LSP-SPP coupling is considered as the major contributor to the sensitivity enhancement, the mass difference between nanoparticles is regarded as another contributor, especially when the LSPR wavelength of the nanoparticle is away from the film SPR wavelength [69]. A more detailed study by Hong and Hall showed that for a 20-nm gold nanoparticle, the dominant enhancement associated with the LSP-SPP coupling effect only occurs when the gap is smaller than  $\sim 8$  nm, while the mass associated with the nanoparticle dominates the enhancement beyond that [70]. Besides the sensitivity consideration, the integrity and stability of the chip should not be ignored in practical sensing situations. As an example, Lumdee et al. developed a robust sensing platform where the gold film was coated with a thin layer of  $\text{Al}_2\text{O}_3$  for both spectral tunability and protection. The sensor chip has demonstrated extreme stability under high-power laser irradiation of 100 W/mm<sup>2</sup> at resonance wavelength [71].

## 6.2 SPR sensing with non-plasmonic nanoparticles

In addition to plasmonic gold and silver nanoparticles, recent reports have shown other choices of nanomaterials for sensitivity enhancement in SPR sensing, such as quantum dots (QDs), graphene, magnetic nanoparticles, hydrogel nanoparticles, and silicon nanoparticles. QDs are semiconductor nanomaterials with a well-known size/composition tunable fluorescent property, and have been widely used in biomedical research for sensing and imaging [72]. With this unique optical property, QDs

have first found applications in the early 2000s for DNA sequence detection using SPR fluorescence spectroscopy [73]. More recently, several ultrasensitive SPR biosensors involving QD-conjugated biomolecules have been developed [74–76]. In 2014, Sandros' group introduced aptamer-modified QDs into an SPRi biosensor and demonstrated a record-high sensitivity of zeptomole ( $10^{-21}$  moles) detection capability for C-reactive protein [77]. The same group had then shown that such an ultrasensitive platform could operate in multiplexed detection for clinical biomarkers [78].

Graphene as a carbon-based 2D material with extraordinary physicochemical properties has found its applications in a wide range of research areas [79]. In SPR sensing, Wu et al. have shown that a thin layer of graphene covering the gold thin film in a conventional SPR sensor would improve the sensitivity due to the increased adsorption of biomolecules on graphene and the optical property of graphene [80]. The adsorption property through  $\pi$ - $\pi$  stacking has also made label-free detection possible. Wang et al. demonstrated a regenerative SPR sensor where aptamers were assembled on the graphene surface and used for  $\alpha$ -thrombin detection [81]. A similar strategy using reduced graphene oxide was later demonstrated in a label-free SPR sensor by Subramanian et al. for selective detection of lysozymes with a detection limit of 0.5 nM [82]. More recently, using phase singularities of the reflected light, Zeng et al. [83] demonstrated an ultralow ssDNA detection limit of  $1 \times 10^{-18}$  M through graphene-gold metasurface architectures. In a conventional SPR sensor chip, it is known that a thin film of silver would generally give a higher sensitivity than gold. However, as silver is more susceptible to harsh environment, gold has remained the first choice. This situation may be changed through graphene coating. According to a numerical simulation from Choi et al. [84] a few layers of graphene on a 60-nm-thick silver film would significantly increase the SPR signal for more than three times. More importantly, the graphene layer also offers great protection against silver oxidation, which was then demonstrated in experiments by Zhao et al. [85].

Similar to graphene, magnetic nanoparticles have also been used in SPR sensors for sensitivity enhancement through analyte enrichment. Teramura et al. first demonstrated the use of 50-nm streptavidin-conjugated magnetic nanobeads to amplify the SPR signal through a sandwich-type immunoassay. Because the SPR signals were highly intensified, the authors were able to detect brain natriuretic peptide at approximately 25 pg/ml [86]. Because of the unique physical property, magnetic nanoparticles not only enrich the concentration of the analyte,

but also have other advantages. Soelberg et al. [87] have shown that with antibody-linked magnetic nanoparticles, one can accomplish the two goals in SPR sensing simultaneously: increasing the sensitivity through concentration enrichment and reducing the background through purification. With these advantages, magnetic nanoparticles have found wide applications in SPR sensing during the past decade [88].

Apart from all the abovementioned nanostructures using analyte enrichment or signal amplification, there are also other means developed for sensitivity enhancement in SPR sensors. Cho et al. introduced hydrogel nanoparticles in SPR microscopy for dynamic monitoring of bioactive peptide melittin uptake. The SPP point diffraction pattern of hydrogel nanoparticles attached to the gold film were recorded and analyzed for quantifying the melittin concentration [89]. Kuo et al. demonstrated that silicon nanoparticles are also capable of enhancing the EM field when coupled with a gold film, which is mainly because of the high refractive index of silicon nanoparticle. More importantly, the enhancement is in the near-infrared region and is polarization dependent. This could have great potential in SPR sensing applications [90]. In addition to using a single type of nanoparticles for sensitivity enhancement, combinations of different

nanomaterials have also been explored. As an example, Wang et al. [91] used a dual signal amplification strategy adopting gold nanoparticle-antibody and antibody-QD conjugates for quantitative detection of biomolecules in clinical samples with high specificity (Figure 7). The dual amplification configuration increased the signal amplification by 50-fold and achieved a detection limit as low as 0.1 ng/ml for  $\alpha$ -fetoprotein, carcinoembryonic antigen, and cytokeratin fragment 21-1.

### 6.3 SPR sensing with nanostructure arrays

As the colloidal synthesis method offers a mass production ability of nanoparticles (at molar scale), plasmonic nanoparticle-based LSPR sensing has great potential in realizing miniaturized and high-throughput biomolecular nanoarrays. However, the variations in the peak-wavelength location because of the constraints in synthesizing monodispersed nanoparticles have limited the screening precision. To reduce the influence from these variations, Guo et al. developed a method to normalize the LSPR from geometrically different nanoparticles. After the normalization, different nanoparticles showed highly consistent plasmon responses and achieved well-fitted

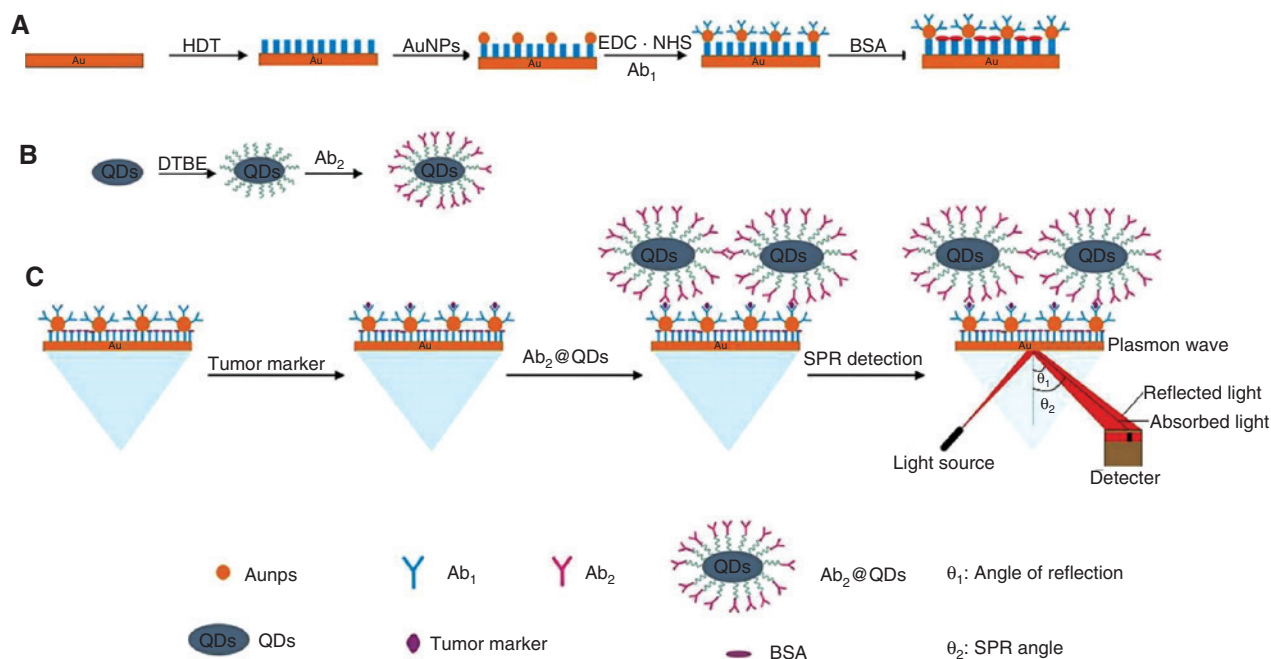


**Figure 7:** Schematic illustration of an SPR biosensor using dual signal amplification strategy. (A) Coating of an SPR chip with  $Ab_1$ @AuNP conjugates. (B) Preparation of  $Ab_2$ @QD conjugates. (C) Sample was flowed along the sensor chip coated with  $Ab_1$ @AuNP conjugates to capture the target, followed by running the  $Ab_2$ @QD conjugates to amplify the signal, which could be detected by the SPR biosensor. Reprinted with permission from Ref. [91].



dose-response curves [92]. Another way to reduce the abovementioned variations is to use lithography methods, such as electron beam lithography, interferometric lithography, and colloidal lithography [93–95]. As compared with colloidal synthesis, lithography offers a much better control over the size, shape, and uniformity of the nanostructures with high precision. Most importantly, it provides the capability of fabricating geometrically ordered nanostructure arrays. With these arrays, SPR could be generated through perpendicular excitation instead of a prism, and thus facilitate the integration of SPR sensor chips [96]. Early demonstrations usually use electron beam lithography for pattern generation. Sharpe et al. demonstrated gold nanohole arrays for immunobiosensing and achieved a spectral response of 393 nm/RIU [97]. Kim et al. then built arrays of nanogratings and nanoholes on a thin gold film for influenza DNA hybridization detection [98]. Using the nanostructure arrays, the angle interrogation-based SPR sensitivity was amplified for 2.54 and 4 times for the nanogratings and nanoholes, respectively. The sensitivity enhancement was found to be attributed to

an increased surface reaction area and stronger coupling between analytes and the excited LSPs. Rodríguez-For-tuño et al. fabricated gold nanocross arrays on silicon substrate for chemical sensing [99]. Owing to the flexibility of electron beam lithography, the parameters of the nanocross structures could be optimized for successful sensing of chemical monolayers with an ultrahigh sensitivity of 500–700 nm/RIU. In general, electron beam lithography could fabricate structures of arbitrary topography with high precision. However, it is usually time consuming and expensive for large-scale fabrication. To overcome this limitation, nanoimprint lithography has been introduced and received great attention. Using this technique, McPhillips et al. [100] fabricated arrays of gold-coated nanodomes on glass substrates. These nanodomes were highly sensitive to the refractive index of the surrounding medium due to their complex plasmonic resonances. In addition, the authors could adjust the array dimensions and the thickness of the gold layer for resonance tuning. Large-scale gold microhole and nanohole arrays as well as silver nanocave arrays have also been fabricated and

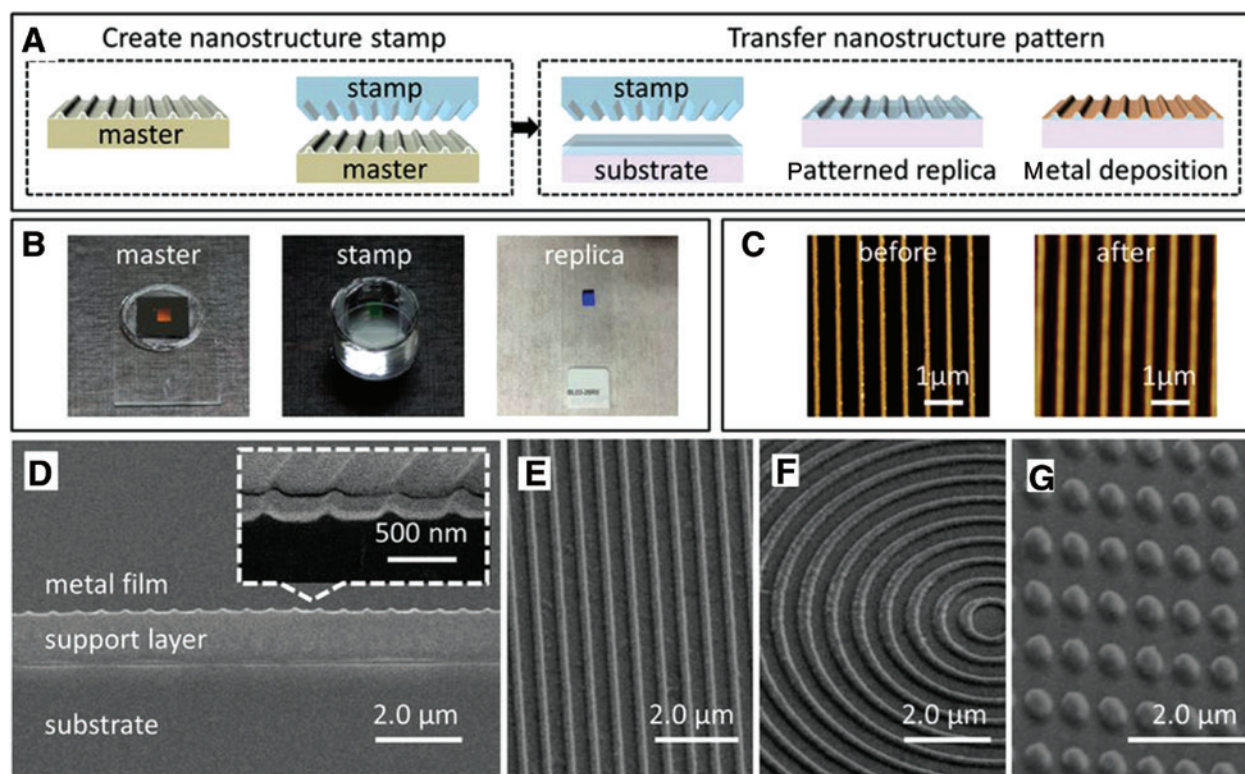


**Figure 8:** Large-scale and high-throughput nanofabrication technique for nanoscale patterns with different designs. Combining the features of nanoimprint and soft lithography, nanostructures could be reproduced rapidly in large amounts for chip devices. (A) Fabrication process flow diagram. (B) Pictures of an EBL patterned master on the silicon substrate, a poly(N,N-dimethylacrylamide) (PDMA) stamp, and a nanostructure replica with a gold thin film layer on a glass slide. (C) Atomic force microscopic images showing the surface morphology of an EBL patterned master (before) and a stamped replica (after). (D). Scanning electron microscopic (SEM) images of a cross section of the structure. (E) A nanograting structure. (F) A bulls-eye structure. (G) A silver array of ~250-nm-diameter nanodots spaced every 600 nm. Reprinted with permission from Ref. [106].

demonstrated for highly sensitive refractive index sensing [101–104]. Dou et al. reported a simple and scalable colloidal lithography technology for fabricating gold nanodons, which demonstrated a high SPR sensitivity of  $\sim 758$  nm/RIU [105]. Combining the features of nanoimprint and soft lithography, Xiao et al. demonstrated a large-scale and high-throughput nanofabrication technique to construct metal thin films with nanoscale patterns of different designs (Figure 8) [106]. Structures such as nanogratings, bulls-eye, and nanodot arrays could be reproduced rapidly in large amounts for chip devices. With these structures, the authors demonstrated label-free SPR sensing with perpendicular transmission configuration using an incoherent white light source. More recently, Aristov et al. [107] reported a 3D plasmonic nanostructure for ultrasensitive biosensing (Figure 9). In their design, a 3D silver-coated woodpile crystal structure was

fabricated by direct laser writing followed by electroless silver plating. By breaking the diffraction-related limitation of 2D periodic structures, the proposed 3D structure showed a delocalized plasmon mode and demonstrated an extremely high spectral sensitivity of  $>2600$  nm/RIU. More importantly, this 3D structure offers a large area for biomolecule immobilization with potential size selectivity option, which enables the implementation of new sensing geometries and strategies that are not feasible with film-based SPR or 2D SPR.

The incorporation of nanoparticles and nanostructures as sensing probes has brought a lot of new opportunities to the conventional SPR sensing technologies. As the typical size of the probes is in the nanometer range, these newly emerged nanoparticle/nanostructure-assisted sensing technologies have enabled us to enter a new regime where localized microscopic changes down to single-molecule level has become accessible. More importantly, recent developments in nanotechnology have provided new tools, such as nanotweezers, to facilitate the manipulation of nanoparticles [108, 109]. With these tools and by combining the imaging techniques, it is now practical to observe the localized molecular interactions and monitor the dynamic process in biological samples with high spatial resolution, sensitivity, and throughput.

## 7 Conclusion

In this review, we summarized the four interrogation modes of intensity, angle, wavelength, and phase in the conventional SPR sensing configuration. Blended in each section of different interrogation modes, recent developments in SPRi technique have been highlighted. The emergence of high-throughput, high-sensitivity, and real-time SPRi methods enables SPR biosensors to perform multiplex sensing of different target analytes with the highest sensitivity. However, the requirement of high throughput also brings the new challenges: (i) fast measurement of the SPR dip in the angle and wavelength interrogation SPRi; (ii) improvement in the performance of the SPRi sensors such as sensitivity, spatial resolution, and dynamic detection range; and (iii) miniaturizing the SPR instruments. Table 1 shows the typical performances of SPR sensors based on intensity, angular, wavelength, and phase interrogations. It can be seen that phase interrogation SPR sensors offer better sensitivity, yet the angular and wavelength interrogation SPR sensors offer better dynamic detection range.

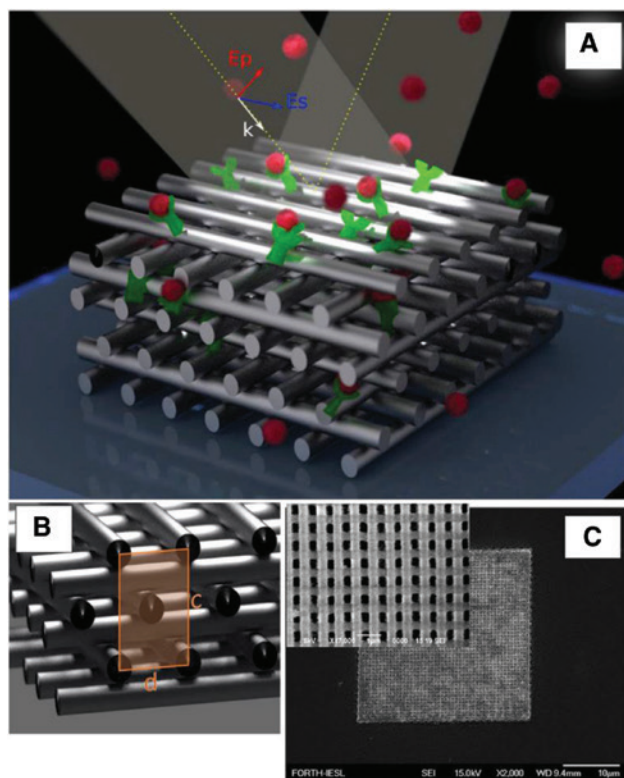


**Figure 9:** A 3D plasmonic metamaterial nanoarchitecture offering a large area for biomolecule immobilization with a much improved spectral sensitivity of 2600 nm/RIU. The structure is based on Ag-coated woodpile crystal produced by multiphoton laser polymerization, followed by Ag-based metallization. (A) Schematic illustration of biosensing using the metamaterial. A receptor (green) is immobilized inside the woodpile structure and its selective partner (red) binds to the receptor sites, leading to a change of parameters for the reflected light. (B) Schematic representation of a woodpile crystal. (C) SEM image of the structure. Reprinted with permission from Ref. [107].

Table 1: Brief comparison between various schemes in SPR sensing.

Interrogation strategies	Sensitivity (RIU)		Dynamic detection range (RIU)		SPRi speed (fps)	Signal processing
	Theoretical	Point	Theoretical	Imaging		
Intensity mode	$\sim 10^{-7}$ (@0.1%)	$2 \times 10^{-6}$ [31]	0.05	$5 \times 10^{-6}$ [110]	Video rate	Simple
Angle mode	$\sim 10^{-8}$ (@0.0001deg)	$3 \times 10^{-8}$ [19]	>0.1	$1 \times 10^{-6}$ [2]	10 [2]	Medium
Wavelength mode	$\sim 10^{-7}$ (@0.001 nm)	$1.8 \times 10^{-7}$ [111]	>0.1	$1.27 \times 10^{-6}$ [104]	2.8 [104]	Medium
Phase mode	$\sim 10^{-9}$ (@0.01 deg)	$2 \times 10^{-8}$ [44]	$10^{-4a}$	$2.7 \times 10^{-7}$ [52]	0.03 [30]	Complex

<sup>a</sup>The theoretical dynamic detection range of the phase interrogation mode with the incident wavelength and angle fixed is about  $10^{-4}$  RIU. The dynamic detection range can be improved through combining the wavelength or angle scanning techniques.

During the past decades, continuous engineering efforts have been made to improve the overall performance of SPR sensors. To further push the limits, state-of-the-art engineering methods are expected. The phase-sensitive SPRi sensor with wavelength multiplexing approach we recently proposed has shown that the combination of different interrogation modes with the imaging technique could be a promising solution. Other than the performance, the portability of SPR sensors is another important consideration. In this respect, an all solid-state scheme with no mechanical moving parts is most possible to produce portable SPR instruments for achieving its full potential.

In recent years, the fast developments in biomedical research have shown great demand for biosensing with high sensitivity, specificity, and throughput. To detect the interactions between specific biomolecules, biosensors with ultrahigh sensitivity down to single molecules and high recognition specificity are expected. In this contribution, we have also reviewed the vast developments in nanotechnology-associated SPR sensing for sensitivity enhancements during the past few years. With the help of colloidal synthesized nanomaterials as well as lithography patterned nanostructures, different approaches have been demonstrated to enhance the sensitivity of conventional SPR sensors of different interrogation modes through EM field enhancement, analyte immobilization, and enrichment. These advancements show that the integration of nanotechnology into SPR sensors has opened the microscopic regime for the conventional SPR sensing down to single-cell or even single-molecule level. With recent advancements in nanotechnology such as plasmonic nanotweezers and super-resolution imaging, we believe that the incorporation of these newly emerged nanotechnology approaches into SPRi technology could bring lots of promising opportunities for future developments in biosensing applications.

**Acknowledgments:** This work was partially supported by the National Major Scientific Research Instruments and Equipment Development Project from National Natural Science Foundation of China (61527827); National Basic Research Program of China (2015CB352005); Guangdong Natural Science Foundation and Province Project (2014A030312008, 2015KGJHZ002, 2015A020214023); Shenzhen Science and Technology R&D Foundation (JCYJ20160422151611496, JCYJ20150324141711698); and Collaborative Research Fund (CRF) (CUHK1/CRF/12G) from the Hong Kong Research Grants Council, Innovation, and Technology Fund (ITF) (GHP/014/13SZ) from the Hong Kong Innovation and Technology Commission.



## References

- [1] Christopher L, Zhiyuan H, Leroy H, Charles TC. SPR imaging for high throughput, label-free interaction analysis. *Comb Chem High Throughput Screen* 2009;12:741–51.
- [2] VanWiggeren GD, Bynum MA, Ertel JP, et al. A novel optical method providing for high-sensitivity and high-throughput biomolecular interaction analysis. *Sens Actuators B Chem* 2007;127:341–9.
- [3] Homola J, Yee SS, Gauglitz G. Surface plasmon resonance sensors: review. *Sens Actuators B Chem* 1999;54:3–15.
- [4] Berger CEH, Beumer TAM, Kooyman RPH, Greve J. Surface plasmon resonance multisensing. *Anal Chem* 1998;70:703–6.
- [5] Löfås S, Malmqvist M, Rönnerberg I, Stenberg E, Liedberg B, Lundström I. Bioanalysis with surface plasmon resonance. *Sens Actuators B Chem* 1991;5:79–84.
- [6] Rothenhausler B, Knoll W. Surface-plasmon microscopy. *Nature* 1988;332:615–7.
- [7] Thiel AJ, Frutos AG, Jordan CE, Corn RM, Smith LM. In situ surface plasmon resonance imaging detection of DNA hybridization to oligonucleotide arrays on gold surfaces. *Anal Chem* 1997;69:4948–56.
- [8] Laplatine L, Leroy L, Calemczuk R, et al. Spatial resolution in prism-based surface plasmon resonance microscopy. *Opt Express* 2014;22:22771–85.
- [9] Wegner GJ, Lee HJ, Marriott G, Corn RM. Fabrication of histidine-tagged fusion protein arrays for surface plasmon resonance imaging studies of protein-protein and protein-DNA interactions. *Anal Chem* 2003;75:4740–6.
- [10] Smith EA, Erickson MG, Uliasz AT, Weisblum B, Corn RM. Surface plasmon resonance imaging of transcription factor proteins: interactions of bacterial response regulators with DNA arrays on gold films. *Langmuir* 2003;19:1486–92.
- [11] Piliarik M, Vaisocherová H, Homola J. A new surface plasmon resonance sensor for high-throughput screening applications. *Biosens Bioelectron* 2005;20:2104–10.
- [12] Abadian PN, Kelley CP, Goluch ED. Cellular analysis and detection using surface plasmon resonance techniques. *Anal Chem* 2014;86:2799–812.
- [13] Yanase Y, Hiragun T, Kaneko S, Gould HJ, Greaves MW, Hide M. Detection of refractive index changes in individual living cells by means of surface plasmon resonance imaging. *Biosens Bioelectron* 2010;26:674–81.
- [14] Sereda A, Moreau J, Canva M, Maillart E. High performance multi-spectral interrogation for surface plasmon resonance imaging sensors. *Biosens Bioelectron* 2014;54:175–80.
- [15] Huang YH, Ho HP, Wu SY, Kong SK. Detecting phase shifts in surface plasmon resonance: a review. *Adv Opt Technol* 2012;2012:471957.
- [16] Mohanty BC, Kasiviswanathan S. Two-prism setup for surface plasmon resonance studies. *Rev Sci Instrum* 2005;76:033103.
- [17] Sathiyamoorthy K, Ramya B, Murukeshan VM, Sun XW. Modified two prism SPR sensor configurations to improve the sensitivity of measurement. *Sens Actuators A Phys* 2013;191:73–7.
- [18] Dougherty G. A compact optoelectronic instrument with a disposable sensor based on surface plasmon resonance. *Meas Sci Technol* 1993;4:697–9.
- [19] Tao N, Boussaad S, Huang W, Arechabaleta R, D'Agnese J. High resolution surface plasmon resonance spectroscopy. *Rev Sci Instrum* 1999;70:4656–60.
- [20] Berger CEH, Greve J. Differential SPR immunosensing. *Sens Actuators B Chem* 2000;63:103–8.
- [21] Wolf LK, Fullenkamp DE, Georgiadis RM. Quantitative angle-resolved SPR imaging of DNA-DNA and DNA-drug kinetics. *J Am Chem Soc* 2005;127:17453–9.
- [22] Wolf LK, Gao Y, Georgiadis RM. Kinetic discrimination of sequence-specific DNA-drug binding measured by surface plasmon resonance imaging and comparison to solution-phase measurements. *J Am Chem Soc* 2007;129:10503–11.
- [23] Ruemmele JA, Golden MS, Gao Y, et al. Quantitative surface plasmon resonance imaging: a simple approach to automated angle scanning. *Anal Chem* 2008;80:4752–6.
- [24] Beusink JB, Lokate AMC, Besselink GAJ, Puijn GJM, Schasfoort RBM. Angle-scanning SPR imaging for detection of biomolecular interactions on microarrays. *Biosens Bioelectron* 2008;23:839–44.
- [25] Zhou C, Jin W, Zhang Y, et al. An angle-scanning surface plasmon resonance imaging device for detection of mismatched bases in caspase-3 DNA. *Anal Methods* 2013;5:2369–73.
- [26] Yuk JS, Kim HS, Jung JW, et al. Analysis of protein interactions on protein arrays by a novel spectral surface plasmon resonance imaging. *Biosens Bioelectron* 2006;21:1521–8.
- [27] Liu L, He Y, Zhang Y, Ma S, Ma H, Guo J. Parallel scan spectral surface plasmon resonance imaging. *Appl Opt* 2008;47:5616–21.
- [28] Chen K, Zeng Y, Wang L, et al. Fast spectral surface plasmon resonance imaging sensor for real-time high-throughput detection of biomolecular interactions. *J Biomed Opt* 2016;21:127003.
- [29] Zeng Y, Wang L, Wu SY, et al. High-throughput imaging surface plasmon resonance biosensing based on an adaptive spectral-dip tracking scheme. *Opt Express* 2016;24:28303–11.
- [30] Wong CL, Ho HP, Suen YK, et al. Real-time protein biosensor arrays based on surface plasmon resonance differential phase imaging. *Biosens Bioelectron* 2008;24:606–12.
- [31] Zybin A, Grunwald C, Mirsky VM, Kuhlmann J, Wolfbeis OS, Niemax K. Double-wavelength technique for surface plasmon resonance measurements: basic concept and applications for single sensors and two-dimensional sensor arrays. *Anal Chem* 2005;77:2393–9.
- [32] Kashif M, Bakar AA, Arsal N, Shaari S. Development of phase detection schemes based on surface plasmon resonance using interferometry. *Sensors* 2014;14:15914–38.
- [33] Nelson SG, Johnston KS, Yee SS. High sensitivity surface plasmon resonance sensor based on phase detection. *Sens Actuators B Chem* 1996;35:187–91.
- [34] Xinglong Y, Lequn Z, Hong J, Haojuan W, Chunyong Y, Shenggen Z. Immunosensor based on optical heterodyne phase detection. *Sens Actuators B Chem* 2001;76:199–202.
- [35] Wu CM, Jian ZC, Joe SF, Chang LB. High-sensitivity sensor based on surface plasmon resonance and heterodyne interferometry. *Sens Actuators B Chem* 2003;92:133–6.
- [36] Chou C, Wu HT, Huang YC, Kuo WC, Chen YL. Characteristics of a paired surface plasma waves biosensor. *Opt Express* 2006;14:4307–15.
- [37] Li YC, Chang YF, Su LC, Chou C. Differential-phase surface plasmon resonance biosensor. *Anal Chem* 2008;80:5590–5.
- [38] Peng HJ, Wong SP, Lai YW, Liu XH, Ho HP, Zhao S. Simplified system based on photoelastic modulation technique for low-level birefringence measurement. *Rev Sci Instrum* 2003;74:4745–9.



- [39] Ho HP, Law WC, Wu SY, et al. Phase-sensitive surface plasmon resonance biosensor using the photoelastic modulation technique. *Sens Actuators B Chem* 2006;114:80–4.
- [40] Yuan W, Ho HP, Wu SY, Suen YK, Kong SK. Polarization-sensitive surface plasmon enhanced ellipsometry biosensor using the photoelastic modulation technique. *Sens Actuators A Phys* 2009;151:23–8.
- [41] Kabashin AV, Nikitin PI. Interferometer based on a surface-plasmon resonance for sensor applications. *Quantum Electron* 1997;27:653–4.
- [42] Kabashin AV, Nikitin PI. Surface plasmon resonance interferometer for bio- and chemical-sensors. *Opt Commun* 1998;150:5–8.
- [43] Wu SY, Ho HP, Law WC, Lin C, Kong SK. Highly sensitive differential phase-sensitive surface plasmon resonance biosensor based on the Mach-Zehnder configuration. *Opt Lett* 2004;29:2378–80.
- [44] Ho HP, Yuan W, Wong CL, et al. Sensitivity enhancement based on application of multi-pass interferometry in phase-sensitive surface plasmon resonance biosensor. *Opt Commun* 2007;275:491–6.
- [45] Ng SP, Loo FC, Wu SY, et al. Common-path spectral interferometry with temporal carrier for highly sensitive surface plasmon resonance sensing. *Opt Express* 2013;21:20268–73.
- [46] Loo FC, Ng SP, Wu CML, Kong SK. An aptasensor using DNA aptamer and white light common-path SPR spectral interferometry to detect cytochrome-c for anti-cancer drug screening. *Sens Actuators B Chem* 2014;198:416–23.
- [47] Nikitin PI, Grigorenko AN, Beloglazov AA, et al. Surface plasmon resonance interferometry for micro-array biosensing. *Sens Actuators A Phys* 2000;85:189–93.
- [48] Xinglong Y, Dingxin W, Xing W, Xiang D, Wei L, Xinsheng Z. A surface plasmon resonance imaging interferometry for protein micro-array detection. *Sens Actuators B Chem* 2005;108:765–71.
- [49] Xinglong Y, Xiang D, Fangfang L, Xing W, Dingxin W. A surface plasmon resonance interferometer based on spatial phase modulation for protein array detection. *Meas Sci Technol* 2008;19:015301.
- [50] Yu X, Ding X, Liu F, Deng Y. A novel surface plasmon resonance imaging interferometry for protein array detection. *Sens Actuators B Chem* 2008;130:52–8.
- [51] Wang D, Ding L, Zhang W, et al. A high-throughput surface plasmon resonance biosensor based on differential interferometric imaging. *Meas Sci Technol* 2012;23:065701–10.
- [52] Shao Y, Li Y, Gu D, et al. Wavelength-multiplexing phase-sensitive surface plasmon imaging sensor. *Opt Lett* 2013;38:1370–2.
- [53] Fong KE, Yung LYL. Localized surface plasmon resonance: a unique property of plasmonic nanoparticles for nucleic acid detection. *Nanoscale* 2013;5:12043–71.
- [54] Maurer T, Adam PM, Lévêque G. Coupling between plasmonic films and nanostructures: from basics to applications. *Nanophotonics* 2015;4:363–82.
- [55] Lévêque G, Martin OJF. Optical interactions in a plasmonic particle coupled to a metallic film. *Opt Express* 2006;14:9971–81.
- [56] Lévêque G, Martin OJF. Tunable composite nanoparticle for plasmonics. *Opt Lett* 2006;31:2750–2.
- [57] Li A, Isaacs S, Abdulhalim I, Li S. Ultrahigh enhancement of electromagnetic fields by exciting localized with extended surface plasmons. *J Phys Chem C* 2015;119:19382–9.
- [58] Golden MS, Bjonnes AC, Georgiadis RM. Distance- and wavelength-dependent dielectric function of Au nanoparticles by angle-resolved surface plasmon resonance imaging. *J Phys Chem C* 2010;114:8837–43.
- [59] Lyon LA, Musick MD, Natan MJ. Colloidal Au-enhanced surface plasmon resonance immunosensing. *Anal Chem* 1998;70:5177–83.
- [60] García-Marín A, Abad JM, Ruiz E, Lorenzo E, Piqueras J, Pau JL. Glutathione immunosensing platform based on total internal reflection ellipsometry enhanced by functionalized gold nanoparticles. *Anal Chem* 2014;86:4969–76.
- [61] Law WC, Yong KT, Baev A, Prasad PN. Sensitivity improved surface plasmon resonance biosensor for cancer biomarker detection based on plasmonic enhancement. *ACS Nano* 2011;5:4858–64.
- [62] Fang S, Lee HJ, Wark AW, Corn RM. Attomole microarray detection of microRNAs by nanoparticle-amplified SPR imaging measurements of surface polyadenylation reactions. *J Am Chem Soc* 2006;128:14044–6.
- [63] Halpern AR, Wood JB, Wang Y, Corn RM. Single-nanoparticle near-infrared surface plasmon resonance microscopy for real-time measurements of DNA hybridization adsorption. *ACS Nano* 2014;8:1022–30.
- [64] Zeng S, Baillargeat D, Ho HP, Yong KT. Nanomaterials enhanced surface plasmon resonance for biological and chemical sensing applications. *Chem Soc Rev* 2014;43:3426–52.
- [65] Burda C, Chen X, Narayanan R, El-Sayed MA. Chemistry and properties of nanocrystals of different shapes. *Chem Rev* 2005;105:1025–102.
- [66] Law WC, Yong KT, Baev A, Hu R, Prasad PN. Nanoparticle enhanced surface plasmon resonance biosensing: application of gold nanorods. *Opt Express* 2009;17:19041–6.
- [67] Kwon MJ, Lee J, Wark AW, Lee HJ. Nanoparticle-enhanced surface plasmon resonance detection of proteins at attomolar concentrations: comparing different nanoparticle shapes and sizes. *Anal Chem* 2012;84:1702–7.
- [68] Maurer T, Nicolas R, Lévêque G, et al. Enhancing LSPR sensitivity of Au gratings through graphene coupling to Au film. *Plasmonics* 2014;9:507–12.
- [69] Mustafa DE, Yang T, Xuan Z, Chen S, Tu H, Zhang A. Surface plasmon coupling effect of gold nanoparticles with different shape and size on conventional surface plasmon resonance signal. *Plasmonics* 2010;5:221–31.
- [70] Hong X, Hall EAH. Contribution of gold nanoparticles to the signal amplification in surface plasmon resonance. *Analyst* 2012;137:4712–9.
- [71] Lumdee C, Yun B, Kik PG. Wide-band spectral control of Au nanoparticle plasmon resonances on a thermally and chemically robust sensing platform. *J Phys Chem C* 2013;117:19127–33.
- [72] Zhou J, Yang Y, Zhang CY. Toward biocompatible semiconductor quantum dots: from biosynthesis and bioconjugation to biomedical application. *Chem Rev* 2015;115:11669–717.
- [73] Robelek R, Niu L, Schmid EL, Knoll W. Multiplexed hybridization detection of quantum dot-conjugated DNA sequences using surface plasmon enhanced fluorescence microscopy and spectrometry. *Anal Chem* 2004;76:6160–5.
- [74] Malic L, Sandros MG, Tabrizian M. Designed biointerface using near-infrared quantum dots for ultrasensitive surface plasmon resonance imaging biosensors. *Anal Chem* 2011;83:5222–9.
- [75] Anderson GP, Glaven RH, Algar WR, et al. Single domain antibody-quantum dot conjugates for ricin detection by both fluoroimmunoassay and surface plasmon resonance. *Anal Chim Acta* 2013;786:132–8.

- [76] Foudeh AM, Daoud JT, Faucher SP, Veres T, Tabrizian M. Sub-femtomole detection of 16s rRNA from *Legionella pneumophila* using surface plasmon resonance imaging. *Biosens Bioelectron* 2014;52:129–35.
- [77] Vance SA, Sandros MG. Zeptomole detection of C-reactive protein in serum by a nanoparticle amplified surface plasmon resonance imaging aptasensor. *Sci Rep* 2014;4:5129.
- [78] Zeidan E, Li S, Zhou Z, Miller J, Sandros MG. Single-multiplex detection of organ injury biomarkers using SPRI based nano-immunosensor. *Sci Rep* 2016;6:36348.
- [79] Chen Y, Tan C, Zhang H, Wang L. Two-dimensional graphene analogues for biomedical applications. *Chem Soc Rev* 2015;44:2681–701.
- [80] Wu L, Chu HS, Koh WS, Li EP. Highly sensitive graphene biosensors based on surface plasmon resonance. *Opt Express* 2010;18:14395–400.
- [81] Wang L, Zhu C, Han L, Jin L, Zhou M, Dong S. Label-free, regenerative and sensitive surface plasmon resonance and electrochemical aptasensors based on graphene. *Chem Commun* 2011;47:7794–6.
- [82] Subramanian P, Lesniewski A, Kaminska I, et al. Lysozyme detection on aptamer functionalized graphene-coated SPR interfaces. *Biosens Bioelectron* 2013;50:239–43.
- [83] Zeng S, Sreekanth KV, Shang J, et al. Graphene-gold metasurface architectures for ultrasensitive plasmonic biosensing. *Adv Mater* 2015;27:6163–9.
- [84] Choi SH, Kim YL, Byun KM. Graphene-on-silver substrates for sensitive surface plasmon resonance imaging biosensors. *Opt Express* 2011;19:458–66.
- [85] Zhao Y, Xie Y, Hui YY, et al. Highly impermeable and transparent graphene as an ultra-thin protection barrier for Ag thin films. *J Mater Chem C* 2013;1:4956–61.
- [86] Teramura Y, Arima Y, Iwata H. Surface plasmon resonance-based highly sensitive immunosensing for brain natriuretic peptide using nanobeads for signal amplification. *Anal Biochem* 2006;357:208–15.
- [87] Soelberg SD, Stevens RC, Limaye AP, Furlong CE. Surface plasmon resonance detection using antibody-linked magnetic nanoparticles for analyte capture, purification, concentration, and signal amplification. *Anal Chem* 2009;81:2357–63.
- [88] Rocha-Santos TAP. Sensors and biosensors based on magnetic nanoparticles. *TrAC Trend Anal Chem* 2014;62:28–36.
- [89] Cho K, Fasoli JB, Yoshimatsu K, Shea KJ, Corn RM. Measuring melittin uptake into hydrogel nanoparticles with near-infrared single nanoparticle surface plasmon resonance microscopy. *Anal Chem* 2015;87:4973–9.
- [90] Kuo YL, Chuang SY, Chen SY, Chen KP. Enhancing the Interaction between high-refractive index nanoparticles and gold film substrates based on oblique incidence excitation. *ACS Omega* 2016;1:613–9.
- [91] Wang H, Wang X, Wang J, Fu W, Yao C. A SPR biosensor based on signal amplification using antibody-QD conjugates for quantitative determination of multiple tumor markers. *Sci Rep* 2016;6:33140.
- [92] Guo L, Ferhan AR, Lee K, Kim DH. Nanoarray-based biomolecular detection using individual Au nanoparticles with minimized localized surface plasmon resonance variations. *Anal Chem* 2011;83:2605–12.
- [93] Chen Y. Nanofabrication by electron beam lithography and its applications: a review. *Microelectron Eng* 2015;135:57–72.
- [94] Xia D, Ku Z, Lee SC, Brueck SRJ. Nanostructures and functional materials fabricated by interferometric lithography. *Adv Mater* 2011;23:147–79.
- [95] Ye X, Qi L. Two-dimensionally patterned nanostructures based on monolayer colloidal crystals: controllable fabrication, assembly, and applications. *NanoToday* 2011;6:608–31.
- [96] Singh P. SPR biosensors: historical perspectives and current challenges. *Sens Actuators B Chem* 2016;229:110–30.
- [97] Sharpe JC, Mitchell JS, Lin L, Sedoglavich N, Blaikie RJ. Gold nanohole array substrates as immunobiosensors. *Anal Chem* 2008;80:2244–9.
- [98] Kim SA, Byun KM, Kim K, et al. Surface-enhanced localized surface plasmon resonance biosensing of avian influenza DNA hybridization using subwavelength metallic nanoarrays. *Nanotechnology* 2010;21:355503.
- [99] Rodríguez-Fortuño FJ, Martínez-Marco M, Tomás-Navarro B, et al. Highly-sensitive chemical detection in the infrared regime using plasmonic gold nanocrosses. *Appl Phys Lett* 2011;98:133118.
- [100] McPhillips J, McClatchey C, Kelly T, et al. Plasmonic sensing using nanodome arrays fabricated by soft nanoimprint lithography. *J Phys Chem C* 2011;115:15234–9.
- [101] Live LS, Dhawan A, Gibson KF, et al. Angle-dependent resonance of localized and propagating surface plasmons in microhole arrays for enhanced biosensing. *Anal Bioanal Chem* 2012;404:2859–68.
- [102] Cheng K, Wang S, Cui Z, Li Q, Dai S, Du Z. Large-scale fabrication of plasmonic gold nanohole arrays for refractive index sensing at visible region. *Appl Phys Lett* 2012;100:253101.
- [103] Zhu J, Bai Y, Zhang L, et al. Large-scale uniform silver nanocave array for visible light refractive index sensing using soft UV nanoimprint. *IEEE Photonics J* 2016;8:1–7.
- [104] Zeng Y, Wang L, Wu SY, et al. Wavelength-scanning SPR imaging sensors based on an acousto-optic tunable filter and a white light laser. *Sensors* 2017;17:90.
- [105] Dou X, Lin YC, Choi B, Wu K, Jiang P. Sensitive surface plasmon resonance enabled by templated periodic arrays of gold nanodonuts. *Nanotechnology* 2016;27:195601.
- [106] Xiao B, Pradhan SK, Santiago KC, Rutherford GN, Pradhan AK. Topographically engineered large scale nanostructures for plasmonic biosensing. *Sci Rep* 2016;6:24385.
- [107] Aristov AI, Manousidaki M, Danilov A, et al. 3D plasmonic crystal metamaterials for ultra-sensitive biosensing. *Sci Rep* 2016;6:25380.
- [108] Wang K, Schonbrun E, Steinvurzel P, Crozier KB. Trapping and rotating nanoparticles using a plasmonic nano-tweezer with an integrated heat sink. *Nat Commun* 2011;2:469.
- [109] Juan ML, Righini M, Quidant R. Plasmon nano-optical tweezers. *Nat Photonics* 2011;5:349–56.
- [110] Campbell CT, Kim G. SPR microscopy and its applications to high-throughput analyses of biomolecular binding events and their kinetics. *Biomaterials* 2007;28:2380–92.
- [111] Chinowsky TM, Quinn JG, Bartholomew DU, Kaiser R, Elkind JL. Performance of the Spreeta 2000 integrated surface plasmon resonance affinity sensor. *Sens Actuators B Chem* 2003;91:266–74.
- [112] Bolduc OR, Live LS, Masson JF. High-resolution surface plasmon resonance sensors based on a dove prism. *Talanta* 2009;77:1680–7.
- [113] Huang YH, Ho HP, Wu SY, Kong SK, Wong WW, Shum P. Phase sensitive SPR sensor for wide dynamic range detection. *Opt Lett* 2011;36:4092–4.